Journal of Organometallic Chemistry, 458 (1993) 211–218

JOM 23662

Ruthenium carbonyl cluster complexes with nitrogen ligands

II *. Syntheses, X-ray structures and interconversion of $Ru_3(\mu\text{-}H)(\mu\text{-}\eta^2\text{-}NC_5H_8)(CO)_{10}$ and $Ru_3(\mu\text{-}H)(\mu_3\text{-}\eta^2\text{-}NC_5H_8)(CO)_9$

Marie P. Cifuentes and Mark G. Humphrey
Department of Chemistry, University of New England, Armidale, N.S.W., 2351 (Australia)

Brian W. Skelton and Allan H. White
Department of Chemistry, University of Western Australia, Nedlands, W.A., 6009 (Australia)

(Received February 15, 1993)

Abstract

The reaction between piperidine and $Ru_3(CO)_{12}$ in refluxing tetrahydrofuran gave the title compounds $Ru_3(\mu\text{-}H)(\mu\text{-}\eta^2\text{-}NC_5H_8)(CO)_{10}$ (1) and $Ru_3(\mu\text{-}H)(\mu_3\text{-}\eta^2\text{-}NC_5H_8)(CO)_9$ (2), both of which have been characterized by means of X-ray diffraction studies, with location and refinement of the core hydrogen atoms. Analysis of the cluster core distances for 1, 2 and related structures suggests that there is substantially more N–C weakening for $\mu_3\text{-}\eta^2$- compared to $\mu\text{-}\eta^2$-coordination. Interconvertibility of 1 and 2 has been demonstrated. Mild thermolysis cleanly converted 1 into 2; the reverse reaction could be quantitatively effected by carbonylation at room temperature. Hydrogenation of 2 effected the elimination of the $\mu_3\text{-}\eta^2$-piperidyl ligand.

1. Introduction

The reactions of $Ru_3(CO)_{12}$ with N-donor ligands continue to attract interest, and have been the subject of a recent review [1]. N-Heterocycles as ligands have been investigated as these have relevance to hydrodenitrogenation modelling; pyridine and its higher homologues are the most persistent of the N-containing impurities in liquid fuels [2]. We have previously reported the reaction between $Ru_3(CO)_{12}$ and pyridine, which afforded the oxidative addition product $Ru_3(\mu\text{-}H)(\mu\text{-}\eta^2\text{-}NC_5H_4)(CO)_{10}$ [3]. We herein report the results of reacting $Ru_3(CO)_{12}$ with piperidine, a possible intermediate in hydrogenation of pyridine, and the characterization by X-ray structural determinations of products incorporating $\mu\text{-}\eta^2$- or $\mu_3\text{-}\eta^2$-piperidyl moieties.

2. Results and discussion

The reaction between $Ru_3(CO)_{12}$ and piperidine in refluxing tetrahydrofuran and subsequent addition of bis(triphenylphosphine)iminium chloride ([ppn]Cl) to the reaction mixture gave four major products on purification by preparative thin layer chromatography. In addition to the known (hydrido)cluster complexes $[ppn][H_3Ru_4(CO)_{12}]$ [4] and $[ppn][HRu_6(CO)_{18}]$ [5] the piperidyl-coordinated clusters $Ru_3(\mu\text{-}H)(\mu\text{-}\eta^2\text{-}NC_5H_8)(CO)_{10}$ (1) and $Ru_3(\mu\text{-}H)(\mu_3\text{-}\eta^2\text{-}NC_5H_8)(CO)_9$ (2) were obtained in yields of 30% and 24%, respectively. Complexes 1 and 2 were isolated as mixtures from chromatography; final purification was achieved through hand sorting of the orange and yellow crystals. These clusters are derived from the partial dehydrogenation of the piperidine ring through activation of the α-carbon-hydrogen bond, affording $\mu\text{-}\eta^2$- and $\mu_3\text{-}\eta^2$- bound iminoyl groups, respectively.

The structure of 1 can be inferred from the spectral data; the ^1H NMR spectrum shows three resonances

---

Correspondence to: Dr. M.G. Humphrey.

* For Part I, see ref. 1.

0022-328X/93/$6.00

© 1993 – Elsevier Sequoia S.A. All rights reserved

due to the methylene protons of the coordinated piperidine at 3.42, 2.68 and 1.64 ppm with relative intensities of 2:2:4, respectively, and a single metal hydride resonance at −14.83 ppm. The ^{13}C NMR spectrum shows 10 resonance lines attributed to the carbonyls between 209 and 185 ppm and four signals between 63 and 20 ppm assigned to the aliphatic carbons of the piperidine ring; the metal-bound carbon was not detected. These data and the mass spectrum parent ion of 666 mass units are consistent with the formulation shown above.

The solid-state structure of **1** is shown in Fig. 1; crystallographic data are given in Table 1, atomic coordinates in Table 2, and selected bond lengths and angles in Table 3. The model adopted in space group $P2_1/m$ is disordered, a full description of the associated refinement problems being given in the Experimental section. The three metal atoms form a triangle with the piperidyl ligand and a hydride bridging the slightly longer Ru–Ru bond. Discussion of the M_3NC core geometry is deferred until later. Average Ru–CO and RuC–O distances (1.91 and 1.14 Å, respectively)

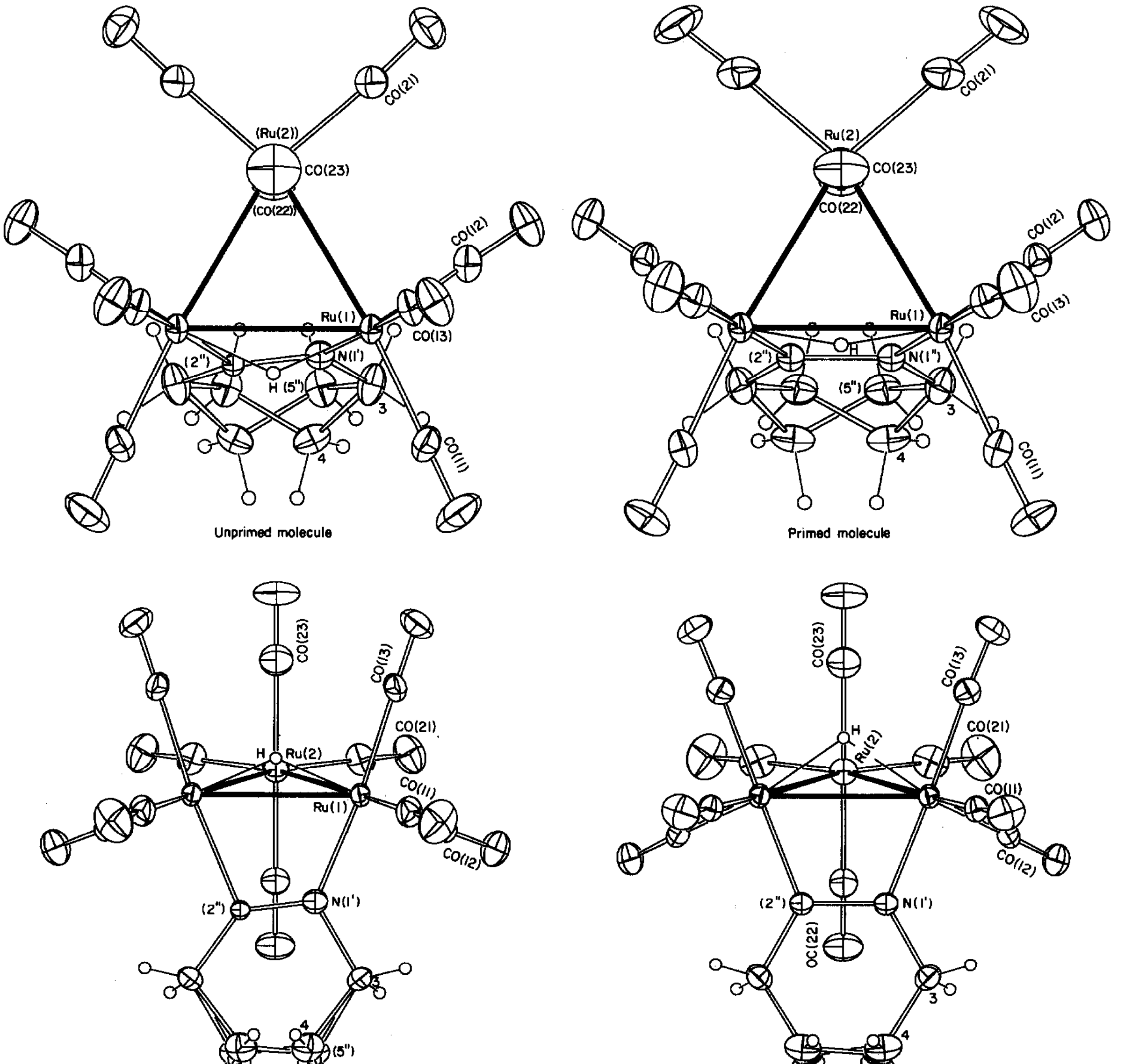

Fig. 1. Molecular structure and crystallographic numbering scheme for $Ru_3(\mu\text{-}H)(\mu\text{-}\eta^2\text{-}NC_5H_8)(CO)_{10}$ (**1**); 20% thermal ellipsoids are shown for the non-hydrogen atoms. Hydrogen atoms have arbitrary radii of 0.1 Å. Projections are shown normal and oblique to the Ru_3 plane for unprimed and primed molecules, both of which have m symmetry. For the unprimed molecule (i), the deconvoluted components of N(1)/C(2) are shown, while for the primed molecule (ii), the average is depicted. Doubly primed atoms are generated by the intramolecular mirror plane.

TABLE 1. Summary of crystallographic data for $Ru_3(\mu\text{-}H)(\mu\text{-}\eta^2\text{-}NC_5H_8)(CO)_{10}$ (1) and $Ru_3(\mu\text{-}H)(\mu_3\text{-}\eta^2\text{-}NC_5H_8)(CO)_9$ (2)

	1	2
Formula	$C_{15}H_9NO_{10}Ru_3$	$C_{14}H_9NO_9Ru_3$
M	666.4	638.4
Crystal system	Monoclinic	Triclinic
Space group	$P2_1/m$ (No. 12)	$P\bar{1}$ (No. 2)
a (Å)	7.464(4)	12.738(3)
b (Å)	15.229(7)	9.807(3)
c (Å)	17.935(11)	7.826(2)
α (°)	90	78.43(2)
β (°)	90.67(5)	82.00(2)
γ (°)	90	82.01(2)
V (Å^3)	2039	942.2
Z	4	2
D_x (g cm^{-3})	2.17	2.25
μ_{Mo} (cm^{-1})	20.3	21.9
Specimen (mm^3)	0.40×0.15×0.13	0.13×0.13×0.45
$A^*_{min,max}$	1.27, 1.38	1.18, 1.40
F(000)	1272	608
θ_{max} (°)	30	32.5
N	6196	6787
N_o	3891	5067
R	0.036	0.039
R_w	0.037	0.041

and RuCO angles (av. 177°) are unexceptional. Distances within the axially coordinated piperidyl ligand (av. 1.51 Å excluding N=C) are also "normal", within the context of its description in terms of a disordered model.

The ^1H NMR spectrum of 2 shows three multiplets in the aliphatic region at 3.59, 3.17 and 1.67 ppm with relative intensities of 2:2:4 and a single metal hydride resonance at −18.02 ppm. The FAB mass spectrum shows the parent ion at 638 mass units and loss of successive CO fragments. The ^{13}C NMR spectrum at room temperature shows three sharp signals between 199 and 193 ppm with relative intensities of 1:6:2 due to the coordinated carbonyls, a signal at 155.7 due to

TABLE 2. Atomic coordinates and equivalent isotropic thermal parameters for $Ru_3(\mu\text{-}H)(\mu\text{-}\eta^2\text{-}NC_5H_8)(CO)_{10}$ (1)

Atom	x	y	z	U_{eq} (Å^2)
Ru(1)	0.60260(5)	0.34479(2)	0.12781(2)	0.0372(1)
Ru(2)	0.43013(8)	1/4	0.01015(3)	0.0444(2)
C(11)	0.7244(8)	0.3990(4)	0.2095(4)	0.060(2)
O(11)	0.7946(7)	0.4312(4)	0.2574(3)	0.109(2)
C(12)	0.4455(8)	0.4394(4)	0.1025(3)	0.057(2)
O(12)	0.3525(6)	0.4965(3)	0.0870(3)	0.087(2)
C(13)	0.7880(7)	0.3829(4)	0.0600(3)	0.054(2)
O(13)	0.9037(6)	0.4069(3)	0.0254(3)	0.089(2)
C(21)	0.3400(9)	0.1553(4)	−0.0482(3)	0.064(2)
O(21)	0.2793(7)	0.1007(3)	−0.0847(3)	0.091(2)
C(22)	0.227(1)	1/4	0.0748(4)	0.052(3)
O(22)	0.0996(7)	1/4	0.1091(4)	0.079(3)
C(23)	0.655(1)	1/4	−0.0406(5)	0.078(4)
O(23)	0.784(1)	1/4	−0.0741(4)	0.115(4)
N(1) [a,b]	0.424(2)	0.205(1)	0.1985(8)	0.045(5)
C(2) [a,b]	0.420(2)	0.290(1)	0.2096(9)	0.027(4)
C(3)	0.3082(8)	0.3452(4)	0.2565(3)	0.060(2)
C(4) [a]	0.246(2)	0.287(1)	0.3248(7)	0.061(5)
C(5) [a]	0.168(2)	0.204(1)	0.2957(8)	0.058(5)
Ru(1′)	0.81935(5)	0.65450(3)	0.40378(2)	0.0386(1)
Ru(2′)	0.95499(8)	3/4	0.28066(3)	0.0474(2)
C(11′)	0.7110(7)	0.6004(4)	0.4894(3)	0.053(2)
O(11′)	0.6434(6)	0.5668(3)	0.5367(3)	0.085(2)
C(12′)	0.9795(7)	0.5640(3)	0.3732(3)	0.049(2)
O(12′)	1.0770(6)	0.5104(3)	0.3567(2)	0.071(2)
C(13′)	0.6260(8)	0.6111(4)	0.3417(3)	0.058(2)
O(13′)	0.5123(6)	0.5822(3)	0.3073(3)	0.094(2)
C(21′)	1.0311(9)	0.8473(5)	0.2179(4)	0.076(3)
O(21′)	1.0756(7)	0.9044(4)	0.1840(3)	0.113(3)
C(22′)	1.178(1)	3/4	0.3361(5)	0.055(3)
O(22′)	1.3144(8)	3/4	0.3651(4)	0.078(3)
C(23′)	0.715(1)	3/4	0.2406(5)	0.067(4)
O(23′)	0.5732(9)	3/4	0.2136(4)	0.094(3)
N(1′) [a,b]	1.017(2)	0.7976(9)	0.4689(8)	0.040(4)
C(2′) [a,b]	1.022(2)	0.714(1)	0.4785(9)	0.031(4)
C(3′)	1.1456(7)	0.6552(4)	0.5193(3)	0.055(2)
C(4′) [a]	1.236(2)	0.705(1)	0.5829(7)	0.062(5)
C(5′) [a]	1.302(2)	0.790(1)	0.5532(7)	0.055(5)
H(1)	0.736(8)	1/4	0.138(3)	0.04(2)
H(1′)	0.68(1)	3/4	0.391(6)	0.14(4)

[a] Site occupancy factor = 0.5. [b] Isotropic thermal parameter.

TABLE 3. Selected bond lengths (Å) and angles (°) for $Ru_3(\mu\text{-}H)(\mu\text{-}\eta^2\text{-}NC_5H_8)(CO)_{10}$ (1) (values are for unprimed and primed molecules, respectively)

Atoms		Bond angle	
Ru(1)–Ru(2)	2.851(1), 2.840(1)	Ru(2)–Ru(1)–Ru(1″)	59.58(2), 59.20(2)
Ru(1)–Ru(1″)	2.887(1), 2.909(1)	Ru(1)–Ru(2)–Ru(1″)	60.83(4), 61.60(4)
Ru(1)–N(1″)	2.00(2), 2.01(1)	Ru(1)–Ru(1″)–N(1)	67.7(5), 68.7(4)
Ru(1)–C(2)	2.18(2), 2.20(2)	C(2)–Ru(1)–Ru(1″)	67.3(4), 65.8(4)
Ru(1)–H	1.76(3), 1.82(6)	N(1)–C(2)–Ru(1)	105(1), 108(1)
N(1)–C(2)	1.30(2), 1.29(2)	C(2)–N(1)–Ru(1″)	119(1), 117(1)
N(1)–C(3″)	1.56(2), 1.49(2)		
C(2)–C(3)	1.46(2), 1.47(2)		
C(3)–C(4)	1.58(2), 1.52(1)		
C(3)–C(5″)	1.47(1), 1.56(1)		
C(4)–C(5)	1.49(2), 1.48(2)		

the metal-bound carbon and four resonances between 68 and 19 ppm due to the aliphatic carbons of the piperidyl ligand. Variable temperature NMR analyses indicate the low temperature limiting spectrum is reached at −80°C and shows the expected nine resonances of the carbonyl carbons between 205.8 and 187.0 ppm (Fig. 2). As the temperature is increased, all resonances except that at 199.5 broaden, such that at −70°C the 4 signals at 193.1–192.3 ppm have averaged to a single resonance. At −50°C, this signal is seen to further coalesce with the resonances at 194.3 and 205.7, finally forming a sharp singlet at 195.1 ppm; the resonances at 200.3 and 187.0 have collapsed into the baseline and coalesce at around −20°C to give the signal at 193.7 ppm.

Fig. 2. Variable temperature ^{13}C NMR spectra for $Ru_3(\mu\text{-}H)(\mu_3\text{-}\eta^2\text{-}NC_5H_8)(CO)_9$ (2).

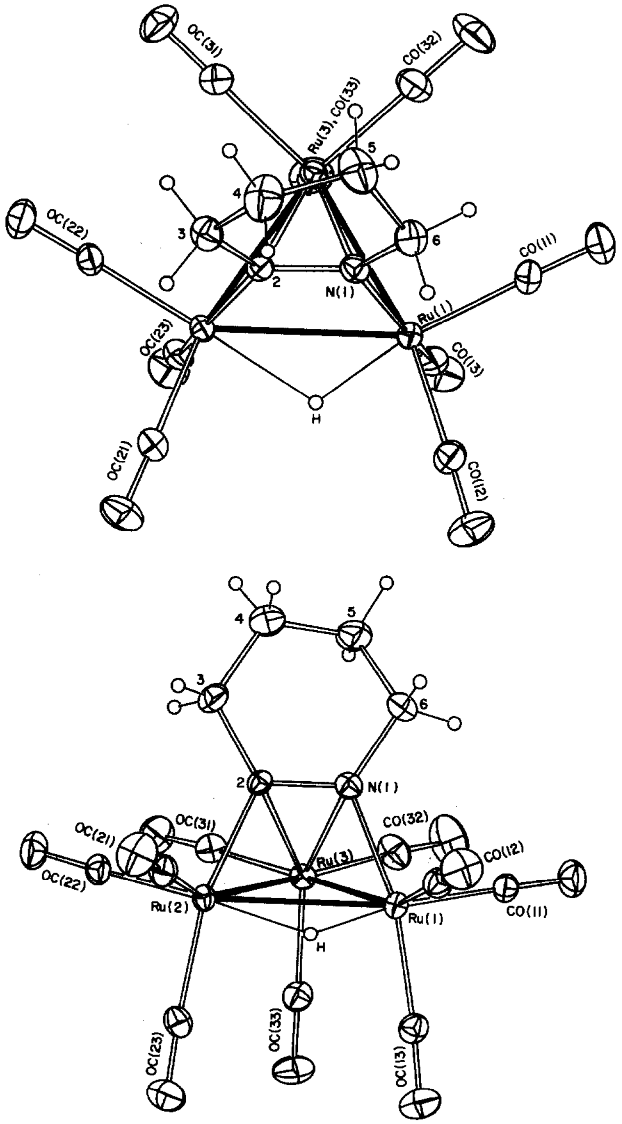

Fig. 3. Molecular structure and crystallographic numbering scheme for $Ru_3(\mu\text{-}H)(\mu_3\text{-}\eta^2\text{-}NC_5H_8)(CO)_9$ (2).

A single-crystal X-ray study was carried out, the result being shown in Fig. 3; crystallographic data are given in Table 1, atomic coordinates in Table 4 and selected bond lengths and angles in Table 5. The three metal atoms form an isosceles triangle with the longest Ru–Ru bond bridged by a hydride and a piperidyl ligand in a μ_3-η^2 mode. The hydride atom was located, with the Ru_2H dihedral angle at 51(2)° to the plane of the ruthenium triangle, and unsymmetrically displaced towards the N-coordinated Ru(1) atom (Ru(1)–H = 1.68(4), Ru(2)–H = 1.94(4) Å). Located hydrido ligands

TABLE 4. Atomic coordinates and equivalent isotropic thermal parameters for $Ru_3(\mu\text{-}H)(\mu_3\text{-}\eta^2\text{-}NC_5H_8)(CO)_9$ (2)

Atom	x	y	z	U_{eq} (Å^2)
Ru(1)	0.10111(3)	0.25849(3)	0.77378(5)	0.0358(1)
Ru(2)	0.29512(3)	0.05750(3)	0.77911(4)	0.0351(1)
Ru(3)	0.28392(3)	0.31176(3)	0.87202(4)	0.0351(1)
C(11)	0.0302(4)	0.4396(5)	0.7859(6)	0.047(2)
O(11)	−0.0146(3)	0.5474(4)	0.7940(5)	0.071(2)
C(12)	0.0110(4)	0.2149(5)	0.6156(7)	0.053(2)
O(12)	−0.0401(4)	0.1891(5)	0.5233(6)	0.086(2)
C(13)	0.0219(4)	0.1792(5)	0.9900(7)	0.048(2)
O(13)	−0.0204(3)	0.1306(4)	1.1198(5)	0.073(2)
C(21)	0.2905(4)	−0.0696(5)	0.6225(7)	0.052(2)
O(21)	0.2901(4)	−0.1455(5)	0.5317(6)	0.086(2)
C(22)	0.4440(4)	0.0169(5)	0.7936(6)	0.046(2)
O(22)	0.5335(3)	−0.0076(4)	0.7974(5)	0.067(2)
C(23)	0.2573(4)	−0.0705(5)	0.9984(7)	0.051(2)
O(23)	0.2330(3)	−0.1388(4)	1.1250(5)	0.074(2)
C(31)	0.4297(4)	0.3083(5)	0.9084(6)	0.049(2)
O(31)	0.5152(3)	0.3028(5)	0.9369(6)	0.077(2)
C(32)	0.2465(5)	0.5033(5)	0.8982(7)	0.060(2)
O(32)	0.2226(4)	0.6134(4)	0.9204(8)	0.108(3)
C(33)	0.2377(4)	0.2275(5)	1.1038(6)	0.048(2)
O(33)	0.2133(3)	0.1800(4)	1.2450(5)	0.070(2)
N(1)	0.2296(3)	0.3370(4)	0.6043(5)	0.041(1)
C(2)	0.3172(3)	0.2425(4)	0.6046(5)	0.033(1)
C(3)	0.4137(4)	0.2718(5)	0.4762(6)	0.052(2)
C(4)	0.4091(5)	0.4086(7)	0.3577(9)	0.085(3)
C(5)	0.3326(5)	0.5179(6)	0.4055(9)	0.083(3)
C(6)	0.2237(4)	0.4713(5)	0.4754(6)	0.053(2)
H	0.141(3)	0.088(4)	0.773(6)	0.05(1)

TABLE 5. Selected bond lengths (Å) and angles (°) for $Ru_3(\mu\text{-}H)(\mu_3\text{-}\eta^2\text{-}NC_5H_8)(CO)_9$ (2)

Atoms		Bond angle	
Ru(1)–Ru(2)	2.9388(7)	Ru(2)–Ru(1)–Ru(3)	57.37(2)
Ru(1)–Ru(3)	2.6990(7)	Ru(2)–Ru(1)–N(1)	67.28(9)
Ru(1)–N(1)	2.090(3)	Ru(2)–Ru(1)–H	39(2)
Ru(1)–H	1.68(4)	Ru(2)–C(2)–N(1)	112.9(3)
Ru(2)–Ru(3)	2.7141(9)	Ru(3)–Ru(1)–N(1)	54.4(1)
Ru(2)–C(2)	2.068(4)	Ru(3)–Ru(1)–H	95(2)
Ru(2)–H	1.94(4)	Ru(3)–Ru(2)–C(2)	55.4(1)
Ru(3)–N(1)	2.254(4)	Ru(3)–N(1)–C(2)	74.4(2)
Ru(3)–C(2)	2.294(4)	Ru(3)–C(2)–N(1)	71.1(2)
N(1)–C(2)	1.348(5)	Ru(1)–Ru(2)–Ru(3)	56.87(2)
N(1)–C(6)	1.490(5)	Ru(1)–Ru(2)–C(2)	67.7(1)
C(2)–C(3)	1.497(6)	Ru(1)–Ru(2)–H	33(1)
C(3)–C(4)	1.469(8)	Ru(1)–N(1)–C(2)	112.1(2)
C(4)–C(5)	1.417(9)		
C(5)–C(6)	1.515(8)		

are rare in structures of this type; in $Ru_3(\mu\text{-}H)(\mu_3\text{-}\eta^2\text{-}CH_3C{=}NCH_2CH_3)(CO)_9$, the hydride was alleged to be "symmetrically disposed" (Ru(1)–H 1.80, Ru(2)–H 1.76 Å) and in the Ru_3 plane, but seemingly was not refined in that determination [6]. The piperidyl ligand is slightly puckered and arranged with the C–N bond almost parallel to the Ru(1)–Ru(2) bond; as with **1**, discussion of the M_3NC core is deferred. Average Ru–CO and RuC–O distances (1.92 and 1.13 Å, respectively) and RuCO angles (av. 178°) are not un-

TABLE 6. Core distances (Å) for $\mu\text{-}\eta^2\text{-}N{=}C\text{–}$ (A) and $\mu_3\text{-}\eta^2\text{-}N{=}C\text{–}$ (B) M_3 structures [a]

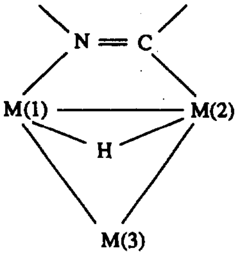

(A)

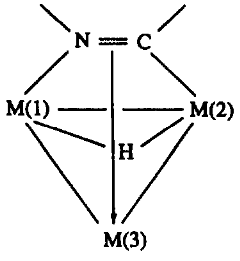

(B)

	A type structures					B type structures			
	1 [b]	**3** [c]	**4** [c]	**5** [d]	**6** [e]	**2** [b]	**7** [f]	**8** [c]	**9** [g]
M(1)–M(2)	2.887(1)	2.9207(4)	2.9496(5)	2.900(1)	2.930(1)	2.9388(7)	3.018(1)	2.9332(8)	2.925(1)
M(1)–M(3)	2.851(1)	2.9115(4)	2.8658(4)	2.864(1)	2.868(1)	2.6990(7)	2.709(1)	2.7222(8)	2.696(1)
M(2)–M(3)	2.851(1)	2.8917(4)	2.8849(5)	2.867(1)	2.870(1)	2.7141(9)	2.709(1)	2.7733(9)	2.720(1)
M(1)–N	2.00(2)	2.093(7)	2.094(7)	2.12(1)	2.12(1)	2.090(3)	2.07(1)	2.13(1)	2.086(5)
M(2)–C	2.18(2)	2.107(7)	2.105(7)	2.14(1)	2.14(1)	2.068(4)	2.07(1)	2.08(1)	2.081(5)
M(3)–N	–	–	–	–	–	2.254(4)	2.26(1)	2.19(1)	2.222(5)
M(3)–C	–	–	–	–	–	2.294(4)	2.26(1)	2.29(1)	2.263(6)
N=C	1.30(2)	1.275(8)	1.29(1)	1.28(2)	1.25(2)	1.348(5)	1.34(1)	1.37(2)	1.343(8)

[a] **3**, $Os_3(\mu\text{-}H)(\mu\text{-}\eta^2\text{-}NC_4H_6)(CO)_9(PPh_3)$ isomer (1); **4**, $Os_3(\mu\text{-}H)(\mu\text{-}\eta^2\text{-}NC_4H_6)(CO)_9(PPh_3)$ isomer (2); **5**, $Os_3(\mu\text{-}H)(\mu\text{-}\eta^2\text{-}CH_3C{=}NCH_3)(CO)_{10}$; **6**, $Os_3(\mu\text{-}H)(\mu\text{-}\eta^2\text{-}NC_4H_6)(CO)_{10}$; **7**, $Ru_3(\mu\text{-}H)(\mu_3\text{-}\eta^2\text{-}NC_4H_6)(CO)_9$; **8**, $Os_3(\mu\text{-}H)(\mu_3\text{-}\eta^2\text{-}CH_3CH_2C{=}NCH_2CH_2CH_3)(CO)_8(PPh_3)$; **9**, $Ru_3(\mu\text{-}H)(\mu_3\text{-}\eta^2\text{-}CH_3C{=}NCH_2CH_3)(CO)_9$. [b] This work. [c] Ref. 7. [d] Ref. 8. [e] Ref. 9. [f] Ref. 10. [g] Ref. 6.

usual. The geometry of the piperidyl ligand in **2** is better defined than in **1**, with peripheral geometry seemingly affected by libration effects.

The M_3NC core distances for **1**, **2** and related Ru and Os complexes are listed in Table 6. For all complexes other than **1**, **2** and **9**, hydrido ligands were placed in calculated positions, bridging M(1)–M(2); this bond is marginally longer than the other intermetallic distances for type **A** complexes, but dramatically longer for complexes of type **B**. Distances M(1)–M(3) and M(2)–M(3) are significantly shorter in **B** type clusters than in **A** type clusters, presumably due to the need to accommodate the face capping ligand. M(1)–N distances are shorter than M(2)–C for complexes **A**, but the reverse is true for complexes **B**. Some asymmetry is apparent for M(3)–ligand distances in **B**; M(3)–N is somewhat shorter than M(3)–C. Consideration of this collected data also substantiates C–N lengthening on moving from **A** to **B** clusters.

Our interest in these clusters stems from their potential as model intermediates for hydrodenitrogenation. While errors associated with N–C distances preclude direct comparison of one structure with another, the accumulated data in Table 6 (μ-η^2-N=C av. 1.27 Å, μ_3-η^2-N=C av. 1.35 Å) suggest that the involvement of the third metal leads to further N=C bond weakening, and argues for the possible intermediacy of μ_3-interactions in the surface-assisted N–C cleavage in hydrodenitrogenation. With this in mind, the hydrogenation of **2** was investigated; a complex mixture resulted in which the major product was found to be $Ru_4(\mu\text{-}H)_4(CO)_{12}$, formed by elimination of the piperidyl moiety, although no evidence of either free piperidine or pentanamine, the ring opening product, was found by GLC analysis of the reaction mixture. Although this result is unclear, we believe that the N–C bond is not sufficiently weakened by μ_3-η^2-coordination, and that the involvement of a fourth metal may be required. Investigations in that direction are currently underway.

Süss-Fink *et al.* have reported that $Ru_3(CO)_{12}$ catalyzes the carbonylation of piperidine, and have isolated the carbamoyl cluster $Ru_3(\mu\text{-}H)(\mu\text{-}\eta^2\text{-}OCNC_5H_{10})(CO)_{10}$ from the reaction mixture [11]; no evidence for the formation of this cluster was found under our reaction conditions. In other related work, Laine and co-workers have reacted $Os_3(CO)_{12}$ with piperidine and obtained $Os_3(\mu\text{-}H)(\mu\text{-}\eta^2\text{-}NC_5H_8)(CO)_{10}$ in about 70% yield [12]; no evidence for an analogue of **2** or higher nuclearity cluster anions was found, consistent with the known lower reactivity and greater stability of the triosmium system.

Isolation of both μ-η^2- and μ_3-η^2-piperidyl clusters from the one reaction suggests that the former is a reaction intermediate en route to the latter. Mild thermolysis of **1** (refluxing cyclohexane, 4 h) effected complete conversion to **2**. The reverse reaction was equally facile; carbonylation of **2** (1 atm, room temperature, 10 min.) afforded **1** cleanly.

3. Experimental

$Ru_3(CO)_{12}$ was synthesized by the low-pressure reaction of $RuCl_3 \cdot xH_2O$ with CO, as previously described [13]. Piperidine and [ppn]Cl were obtained from Hopkin and Williams, and Aldrich, respectively, and used without further purification. Tetrahydrofuran (THF) was distilled from Na/benzophenone under argon prior to use; cyclohexane was dried over Na wire. The reactions were carried out by use of standard Schlenk techniques [14] under an atmosphere of dry argon or carbon monoxide (carbonylation of **2**), although subsequent workup was carried out without any precautions to exclude air. Thin layer chromatography (TLC) was on glass plates (20 × 20 cm^2) coated with Merck GF_{254} silica gel (0.5 mm).

IR spectra were recorded using a Perkin-Elmer model 1725 Fourier-transform spectrophotometer with CaF_2 optics. NMR spectra were recorded on a Bruker AM300 spectrometer, the ^1H spectra at 300.13 MHz, the ^{13}C at 75.47 MHz using approximately 0.04 M $Cr(acac)_3$ as the relaxation agent and a recycle delay of 0.5 s. FAB mass spectra were recorded using a VG ZAB 2HF instrument (exciting gas Ar, source pressure 10^{-6} mbar, FAB gun voltage 7.5 kV, current 1 mA, accelerating potential 8 kV) at the University of Adelaide. The matrix was 3-nitrobenzyl alcohol. Peaks were recorded as *m/z*. Elemental analyses were by the Microanalytical Service in the Department of Chemistry, University of Queensland.

3.1. Reaction of $Ru_3(CO)_{12}$ with piperidine

A solution of piperidine (168 mg, 1.97 mmol) in THF (5 ml) was added to one of $Ru_3(CO)_{12}$ (200 mg, 0.31 mmol) in THF (100 ml) and the mixture refluxed for 4 h. It was then allowed to cool to room temperature, [ppn]Cl (200 mg, 0.36 mmol) was added to the red-brown solution, and the mixture stirred for 15 min. Filtration followed by preparative TLC, with 20% acetone in petrol as eluant, gave four bands. Crystallization of the first and second bands from hexane afforded orange crystals of $Ru_3(\mu\text{-}H)(\mu\text{-}\eta^2\text{-}NC_5H_8)(CO)_{10}$ (**1**) (63 mg, 30%, dec. 162°) and yellow crystals of $Ru_3(\mu\text{-}H)(\mu_3\text{-}\eta^2\text{-}NC_5H_8)(CO)_9$ (**2**) (50 mg, 24%, dec. 122°) respectively, with minor cross-contamination of each complex; final purification required separation of the crystals by hand. The third band contained a small amount of an unidentified red compound; the fourth band was crystallized from

EtOH/hexane to yield red crystals identified from the IR and NMR spectra as a mixture of [ppn][$H_3Ru_4(CO)_{12}$] [4] and [ppn][$HRu_6(CO)_{18}$] [5] (66 mg, approx. 1 : 1, 7%).

3.2. Analytical data

1: Anal. Found: C, 26.34; H, 1.35; N, 1.49%; M^+ 666. $C_{15}H_9NO_{10}Ru_3$ calc.: C, 27.03; H, 1.36; N, 2.10%; M^+ 666. IR (cyclohexane): ν(CO) 2097m, 2058s, 2044s, 2023m, 2006m, 1995m, 1986w, 1982w, 1958w cm^{-1}. ^1H NMR: $\delta(CDCl_3)$ 3.42 (m, 2H); 2.68 (m, 2H); 1.64 (m, 4H); −14.83 (s, 1H). ^{13}C NMR: δ ($CDCl_3$) 208.23, 207.69, 205.61, 201.00, 200.64, 196.17, 191.81, 191.19, 189.98, 186.54 (10 × CO), 62.15 (C6), 46.24 (C3), 23.71 (C5), 20.07 (C4 of piperidyl).

2: Anal. Found: C, 26.47; H, 1.67; N, 1.76%; M^+ 638. $C_{14}H_9NO_9Ru_3$ calc.: C, 26.34; H, 1.42; N, 2.19%; M^+ 638. IR (cyclohexane): ν(CO) 2090m, 2063s, 2034s, 2018s, 2006m, 2003m, 1995m, 1978w, 1972w cm^{-1}. ^1H NMR: $\delta(CDCl_3)$ 3.59 (t, J(HH) = 5.5 Hz (2H)); 3.17 (t, J(HH) = 6.5 Hz (2H)); 1.67 (m, 4H); −18.02 (s, 1H). ^{13}C NMR at 298 K; δ(toluene-d_8) 198.93 (1CO); 195.15 (6CO); 193.68 (2CO); 155.69 (C2); 68.05 (C6); 46.64 (C3); 25.22 (C5); 19.34 (C4 of piperidyl); CO resonances at 193 K: δ(toluene-d_8) 205.78, 200.35, 199.46, 194.62, 193.12, 192.88, 192.59, 192.33, 187.03.

3.3. Conversion of 1 to 2

A solution of **1** (23 mg, 0.036 mmol) was refluxed in cyclohexane (10 ml) for 4 h. The IR spectrum at this stage showed essentially quantitative conversion to **2**.

3.4. Carbonylation of 2

CO was bubbled with stirring through a solution of **2** (10 mg, 0.016 mmol) in cyclohexane (10 ml) at room temperature. An IR spectrum obtained after 10 min showed complete conversion into **1**.

3.5. Hydrogenation of 2

H_2 was bubbled with stirring through a solution of **2** (3 mg, 0.005 mmol) in cyclohexane (10 ml). The temperature was smoothly raised to the reflux point of the solvent, at which point **2** began to disappear with formation of $Ru_4(\mu\text{-}H)_4(CO)_{12}$ (by solution IR). After 7 h, a complex mixture of products was detected by TLC, in which $Ru_4(\mu\text{-}H)_4(CO)_{12}$ was identified as the major product by TLC and IR.

3.6. Structure determination

Single crystals of **1** and **2** suitable for the X-ray work were grown from saturated hexane solution at *ca.* −20°C. Unique diffractometer data sets (2θ–θ scan mode; monochromatic Mo K_α radiation, $\lambda = 0.7107_3$ Å) were measured at ~ 295 K, yielding N independent reflections, N_o of these with $I > 3\sigma(I)$ being considered "observed" and used in the full matrix least squares refinements after gaussian absorption corrections. Anisotropic thermal parameters were refined for the non-hydrogen atoms; $(x, y, z, U_{iso})_H$ for the ligand hydrogen atoms were constrained at estimated values, while those for the core hydrogen atoms were refined. Conventional residuals on $|F|$, R and R_w are quoted, statistical weights derivative of $\sigma^2(I) = \sigma^2(I_{diff}) + 0.0004\sigma^4(I_{diff})$ being used. Neutral atom complex scattering factors were employed; computation used the XTAL 3.0 program system implemented by Hall [15]. Pertinent results are given in the figures and tables; material deposited comprises structure factor amplitudes, thermal and hydrogen parameters and full molecular non-hydrogen geometry.

3.7. Abnormal features / variations in procedure

(1) Space group assignment for this compound must be regarded with considerable circumspection. While of symmetry no higher than monoclinic, but with the β angle close to 90°, systematic absences in the data enable the postulation of a number of possible space group symmetries or pseudo-symmetries, the highest of which is $P2_1/m$, as given. Initial solution and refinement of the structure in this space group, using an extensive data set resulted in an agreeably low residual; in this model, two independent half molecules, relative to their other halves by the $P2/m$ mirror planes comprise the asymmetric unit of the structure. Two of the piperidine ring atoms lie in close association with the Ru_3 cluster, presumed, particularly in view of the analogy of **2**, to be nitrogen and carbon and, in a $P2_1/m$ model, necessarily disordered about the mirror plane. Additional disorder, which may or may not be consequent upon the disorder of the bonded carbon and nitrogen, is found in the remainder of the piperidine ring, with discrete individual components C(4,5) resolvable and refinable, a situation not tenable for C(2) which was modelled as a single atom. The coordinated C/N composite is resolvable into two refinable components, one slightly closer to the Ru_3 core; refinement of population parameters and consideration of associated thermal parameter behaviour was consistent throughout with equal populations of disordered sites and with that atom more closely coordinated to the cluster being assigned as nitrogen. Accordingly, the populations of all disordered components were constrained at 0.5; in the figures, the unprimed molecule is depicted with the individual N(1)/C(2) components deconvoluted, while the primed molecule is shown with joint occupancy of the site. Despite the relatively satisfactory residual, serious reservations remain about the correctness of the space

group, and whether an ordered model in a lower symmetry space group, *e.g.* $P2_1$, involving removal of the constraint of the mirror plane, may not be the true description. Attempts to initiate meaningful refinement with a model of this type proved fruitless, understandably so since the lower symmetry component of the structure is a minor perturbation on a basically centrosymmetric model and inevitably results in correlation problems. Accordingly, conclusions drawn in respect of coordination of the piperidine in particular, but also other associated geometries which will be affected by the superposition and transmission of real or illegitimate concomitant "disorder" throughout the rest of the model, should be regarded with suitable caution. Notwithstanding the above, "meaningful" refinement of the core hydrogen atom was possible, confirming, at least, its presence.

(2) By contrast, solution of this structure was unambiguous and unproblematical, with meaningful refinement of the core hydrogen atom, and confident assignment of coordinated nitrogen and carbon. No disorder is evident.

Acknowledgements

We thank the Australian Research Council for support of this work, and Dr C. Adams for the FAB mass spectra. We also thank Johnson-Matthey Technology Centre for the generous loan of $RuCl_3 \cdot xH_2O$. M.P.C. holds a University of New England Postgraduate Research Award.

References

1 M.I. Bruce, M.P. Cifuentes and M.G. Humphrey, *Polyhedron, 10* (1991) 227.

2 J.R. Katzer and R. Sivasubramanian, *Catal. Rev.-Sci. Eng., 25* (1983) 459.

3 M.I. Bruce, M.G. Humphrey, M.R. Snow, E.R.T. Tiekink and R.C. Wallis, *J. Organomet. Chem., 314* (1986) 311.

4 K.E. Inkrott and S.G. Shore, *Inorg. Chem., 18* (1979) 2817.

5 C.R. Eady, B.F.G. Johnson, J. Lewis, M.C. Malatesta, P. Machin and M. McPartlin, *J. Chem. Soc., Chem. Commun.*, (1976) 945.

6 S. Aime, R. Gobetto, F. Padovan, M. Botta, E. Rosenberg and R.W. Gellert, *Organometallics, 6* (1987) 2074.

7 M. Day, D. Espitia, K.I. Hardcastle, S.E. Kabir, E. Rosenberg, R. Gobetto, L. Milone and D. Osella, *Organometallics, 10* (1991) 3550.

8 S.K. Kabir, M. Day, M. Irving, T. McPhillips, H. Minassian, E. Rosenberg and K.I. Hardcastle, *Organometallics, 10* (1991) 3997.

9 E. Rosenberg, S.E. Kabir, K.I. Hardcastle, M. Day and E. Wolf, *Organometallics, 9* (1990) 2214.

10 M. Day, S. Hajela, S.E. Kabir, M. Irving, T. McPhillips, E. Wolf, K.I. Hardcastle, E. Rosenberg, L. Milone, R. Gobetto and D. Osella, *Organometallics, 10* (1991) 2743.

11 G. Süss-Fink, M. Langenbahn and T. Jenke, *J. Organomet. Chem., 368* (1989) 103.

12 A. Eisenstadt, C.M. Giandomenico, M.F. Frederick and R.M. Laine, *Organometallics, 4* (1985) 2033.

13 M.I. Bruce, C.M. Jensen and N.L. Jones, *Inorg. Synth., 26* (1989) 259.

14 D.F. Shriver and M.A. Drezdzon, *The Manipulation of Air Sensitive Compounds*, 2nd edition, Wiley, New York, 1986.

15 S.R. Hall and J.M. Stewart (eds.), *The XTAL 3.0 Reference Manual*, Universities of Western Australia and Maryland, 1990.